J|A|C|S
ARTICLES
Published on Web 01/20/2004

Kinetic Inhibitor of Hydrate Crystallization

Mark T. Storr,[†,‡] Paul C. Taylor,[†] Jean-Pierre Monfort,[§] and P. Mark Rodger*[,†]

Contribution from the Department of Chemistry, The University of Warwick, Coventry CV4 7AL, United Kingdom

Received March 20, 2003; E-mail: p.m.rodger@warwick.ac.uk

Abstract: We present the results of a combined theoretical/experimental study into a new class of kinetic inhibitor of gas hydrate formation. The inhibitors are based on quaternary ammonium zwitterions, and were identified from a computational screen. Molecular dynamics simulations were used to characterize the effect of the inhibitor on the interface between a type II hydrate and natural gas. These simulations show that the inhibitor is bifunctional, with the hydrophobic end being compatible with the water structure present at the hydrate interface, while the negatively charged functional group promotes a long ranged water structure that is inconsistent with the hydrate phase; the sulfonate-induced structure was found to propagate strongly over several solvation shells. The compound was subsequently synthesized and used in an experimental study of both THF and ethane hydrate formation, and was shown to have an activity that was comparable with an existing commercial kinetic inhibitor: PVP.

1. Introduction

Clathrate hydrates are a type of inclusion compound in which a host lattice of water molecules entraps one or more other molecular species, the 'guest'. The water lattice is a tetrahedral hydrogen bond network containing at least two types of polyhedral cavities. These cavities (or cages) can accommodate a variety of guest species. Probably the most important category of guests—the small nonpolar or weakly polar molecules such as CH_4, C_2H_6, Ar, Kr, Xe, N_2, H_2S, and CO_2—are gases in their standard state and hence clathrate hydrates are often referred to as gas hydrates.

Gas hydrate formation is a concomitant process requiring the presence of both the host and guest molecular species. Conditions under which hydrates will form are determined largely by the nature of the guest, but for most common components of natural gas they will crystallize at temperatures above the ice point with pressures $\sim 10^1$ atm. Such conditions are sufficiently common in geological settings that methane hydrate, in particular, is believed to be the most abundant naturally occurring form of methane.[1] Such conditions are also common in oil and gas transmission, and so gas hydrate formation is a major potential cause of pipeline occlusion; this was first recognized as long ago as 1934.[2]

Currently, the only viable way of avoiding hydrate blockages in oil and gas pipelines is to use chemical inhibitors. These may be of two kinds: thermodynamic or "low dosage" (TIs and LDIs, respectively). The TIs include compounds such as methanol or glycols and act by shifting the water/hydrocarbon/hydrate three-phase equilibrium line. Because they tend to be water soluble, TIs are required at very high concentrations (up to 50 wt % water) and consequently cost the industry ca. $500 million per year.[3] The LDIs can also be split into two closely related groups: kinetic inhibitors (KIs) and anti-agglomerants (AAs). Both provide an attractive alternative as they are active at concentrations below 1 wt % water.[4] The KIs were first considered about 15 years ago. Their effect is to delay the onset of nucleation or slow the growth rate of any crystals that do form, so that fluid flow can be maintained during those finite intervals that oil or gas flow occurs within the hydrate forming region of the phase diagram. AAs, on the other hand, do not prevent hydrate formation, but ensure that hydrates form a finely suspended slush so that fluid flow is not impeded. Activity in both kinds of LDI is believed to arise in a manner similar to that found for anti-freeze proteins:[5] selective adsorption of the inhibitor onto specific crystal growth surfaces disrupts further growth of the hydrate or aggregation of hydrate particles.[6] Indeed, a number of simulation studies have invoked this working hypothesis to try to develop a computational screen for new KIs.[7,8] However, while some correlation between surface adsorption calculations and activity can be expected due to residual structure in the interfacial region,[9] the model should be recognized as a useful simplification.[10]

† Department of Chemistry, The University of Warwick.
‡ Present address: Department of Chemistry, University of Reading, Reading RG6 2AD, U.K.
§ ENSIACET and LGC, 118 route de Narbonne, 31077 Toulouse Cedex 4, France.

(1) Sloan, E. D. *Clathrate Hydrates of Natural Gases*, 2nd ed.; Marcel Dekker: New York, 1998.
(2) Hammerschmidt, E. G. *Ind. Eng. Chem.* **1934**, *26*, 851.
(3) Sloan, F. P.; Subramanian, S.; Matthews, P. N.; Lederhos, J. P.; Khokar, A. A. *Ind. Eng. Chem. Res.* **1998**, *37*, 3124.
(4) Notz, P. K.; Bumgartner, S. B.; Schaneman, J. L.; Todd, B. D. The Application of kinetic Inhibitors to Gas Hydrate Problems, *Offshore Technology Conference*, Houston, USA, 1−4 May, 1995.
(5) Lal, M.; Clark, A. H.; Lips, A.; Ruddock, J. N.; White D. N. J. *Faraday Discussions* **1993**, *95*, 299.
(6) Phillips, N. J.; Kelland, M. A. In *Industrial Applications of Surfactants*; Karsa, D. R., Ed.; Royal Society of Chemistry, 1999, pp 244−259.
(7) Freer, E. M.; Sloan, E. D. *Annal. N. Y. Acad. Sci.* **2000**, *912*, 651.
(8) Makogon, T. Sloan, E. D. *Proc. 4th Int. Conf. Gas Hydrates, Yokohama* **2003**, 498.
(9) Rodger, P. M. *Annal. N. Y. Acad. Sci.* **2000**, *912*, 474.

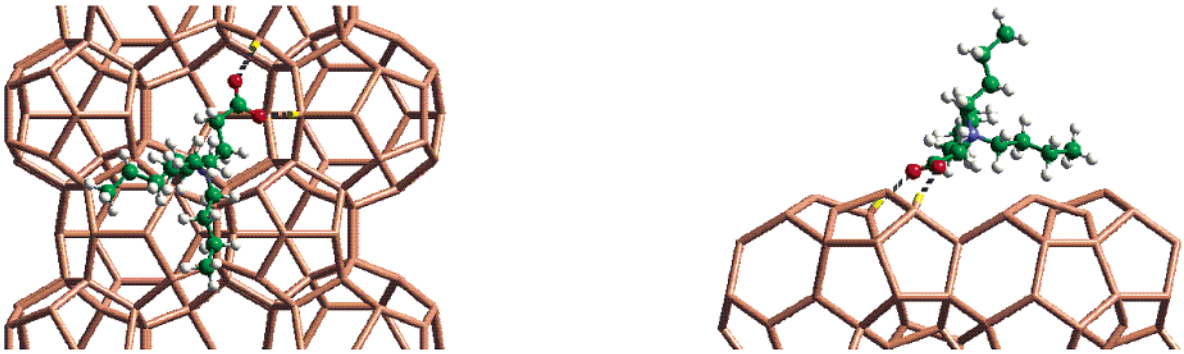

Figure 1. Top (left) and side (right) views of a Zwitterionic LDI capping a large pothole on the static surface of a type II hydrate.

A large number of different chemical motifs have been explored in the search for new LDIs. In general, the successful KIs are polymeric and usually involve small cyclic amide groups such as pyrrolidone or capralactam as the active unit.[11] Quaternary ammonium ions have also been used, both as AAs (with long alkyl chains) or in blends to improve the activity of KIs.[12] Various common surfactants have been considered, although these can cause additional problems due to foaming.[13] Currently available KIs can prevent hydrate formation for a period of days at up to about 13 °C subcooling, whereas AAs can allow up to 20 °C subcooling.[14] However, many applications require larger subcooling, and so developing new LDIs that will give increased subcooling at lower concentrations is still a major interest in the oil and gas industry.

In this paper we present the results of a combined theoretical/experimental characterization of a new KI: tributylammonium-propylsulfonate, or TBAPS (**1**). The possible activity of this compound was suggested from the results of a computational screening program, which indicated that the bifunctional nature of this compound with respect to both charge and to hydrophobic/hydrophilic balance created a novel recognition motif for hydrate surfaces.[15] It was then used in molecular dynamics (MD) simulations of a hydrate/hydrocarbon gas interface under conditions where the hydrate is expected to be stable. We report here an analysis of these simulations aimed at identifying the molecular basis for activity. The compound was then subjected to experimental trials and found to have comparable activity to one of the KIs commonly used as a reference standard, namely poly(vinylpyrrolidone) (PVP). More extensive testing, and comparison with more active KIs, is in progress.[16]

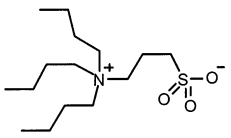

1 tributylammoniumpropylsulfonate

The paper is structured as follows. Section 2 describes the basis on which **1** was identified as a potential KI for hydrate formation. This is followed by a discussion of the MD study carried out to characterize the molecular basis for KI activity. Finally, we report experiments performed with **1** on both tetrahydrofuran (THF) and ethane hydrate.

2. Identification of a New Kinetic Inhibitor

The possibility that quaternary ammonium zwitterions might show interesting properties as KIs emerged from an earlier computational screening study.[15] The methods employed in this study have been described elsewhere[17,18] and so are summarized only briefly here. Metropolis Monte Carlo (MC) simulations were used to examine the interaction of a single molecular species (a possible active unit for a KI) with a set of surfaces that had previously been identified as the most important for growth of a type II hydrate.[17,19] The surfaces were kept rigid and trial translations and rotations applied to a rigid KI; different KI conformations were considered in separate simulations. Each simulation involved 10^6 MC moves, which was sufficiently long to ensure that the distribution of KI center of mass positions both sampled the whole surface and did not change when the simulation time was doubled. These simulations were then analyzed to identify characteristic adsorption modes and geometries. The growth surfaces of a type II hydrate exhibit complex topologies with identifiable islands and many pot-holes up to ca. 7 Å in depth.[17] The potholes arise from the partially formed cages found on the surface, and were usually found to be the favored site for adsorption of a KI monomeric unit. In particular, the amide-based KIs were found to adsorb with the amide side chain located inside the pothole, the amide oxygen hydrogen bonding to the hydrate surface, and the polymer backbone located above the surface.[17,20] A rather different binding motif was found with the quaternary ammonium zwitterions, however: in this case, the additive did not occupy the surface potholes, but instead crated a "lid" for them, with strong hydrogen bonding interactions between the hydrate surface and both the cationic and anionic centers causing the additive to cover the top of the pothole (Figure 1). The interaction energies were indicative of a recognition process, with strong binding found only when the cages showed the

(10) Carver, T. J.; Drew, M. G. B.; Rodger, P. M. *J. Chem. Soc., Faraday Trans.* **1995**, *91*, 3449; Carver, T. J.; Drew, M. G. B.; Rodger P. M. *J. Chem. Soc., Faraday Trans.* **1996**, *92*, 5029.
(11) Freer, E. M.; Sloan, E. D. *Ann. N. Y. Acad. Sci.* **2000**, *912*, 651.
(12) Klomp, U. C., Reinjhart, R. B., patent WO96/34177, 1996; Klomp, U. C. patent WO99/13197, 1999.
(13) Rabeony, M.; Peiffer, D. G.; Costello, C. A.; Wright, P. J.; Colle, K. S.; Talley, L. D. patent WO96/8636, 1996; Anselme M. J.; Reinjhout M. J.; Muijs, H. M.; Klomp, U. L., patent EP0457375A1, 1991.
(14) Argo, C. B.; Berger, R.; Shoup, G.; Fleyfel, F.; Andersson, V.; Larsen, R.; *Proc. 4th Int. Conf. Gas Hydrates, Yokohama* **2003**, 873.
(15) Storr, M. T., MSc Thesis, University of Reading, **1997**.
(16) Di Salvo, A. F.; Taylor, P. C.; Arjmandi, M.; Ren, S. R.; Todd, A. C.; Tohidi, B.; Rodger, manuscript in preparation.
(17) Carver, T. J.; Drew, M. G. B.; Rodger, P. M. *J. Chem. Soc., Faraday Trans.* **1996**, *92*, 5029.
(18) Storr, M. T.; Rodger, P. M.; Monfort, J.-P.; Jussaume, L. *AIChE Symp. Ser.* **2001**, *97*, 256.
(19) Smelik, E. A.; King, H. E. *Am. Mineral.* **1997**, *82*, 88.
(20) Carver, T. J.; Drew, M. G. B.; Rodger, P. M. *Ann. N. Y. Acad. Sci.* **2000**, *912*, 658.

appropriate topology and pattern of dangling water hydrogen atoms to act as hydrogen bond donors. This mode of binding was sufficiently different from that of most other KI motifs (including small cyclic amides such as pyrrolidone and capralactam) to suggest that these compounds might have interesting properties as KIs. As a direct result, **1** was employed in an MD study of a hydrate/hydrocarbon interface, subsequently synthesized and then used in experiments to determine its effect on the induction time, growth rate and morphology of hydrate crystallization.

3. Molecular Dynamics Simulations of an Inhibited Interface

3.1 Simulation Details. *NVT* MD calculations were conducted using DL_POLY.[21] Water was modeled using the SPC potential[22] and methane or propane with united atom potentials.[23] This combination of parameters have been found to give an accurate description of methane hydrate in previous studies.[24] The TBAPS was modeled using an all-atom CHARMm forcefield,[25] and Lorenz−Berthelot mixing rules for the cross parameters. All short-range interactions were truncated at 9.5 Å, whereas the Ewald method[26] was used to evaluate electrostatic interactions [$\alpha = 0.210$ Å^{-1}, $\boldsymbol{k}_{max} = (3, 4, 11)$].

A hydrate surface was constructed using a method described previously.[17] This amounted to creating a $21.20 \times 24.48 \times 29.98$ Å ($x \times y \times z$) orthorhombic supercell containing 408 water molecules and oriented such that the z direction was along the crystallographic (111) direction. Oxygen positions were taken from the experimental structure[27] and hydrogen atoms placed in a manner consistent with the 2-fold crystallographic disorder. Periodic boundaries were used in the $x-y$ plane to give an infinite thin film. The displacement of the cell along the (111) direction was such as to give the (111; −0.001) surface that had previously been identified as the most active cleavage plane for hydrate KIs.[17]

A methane/propane mixture was then added to the system. Initially, one methane molecule was placed in each small cage and one propane molecule in each large cage, giving a total of 48 methane and 24 propane molecules within the hydrate film. Then the z dimension of the simulation cell was increased to 72.6 Å and a mixture of 120 propane and 200 methane molecules inserted in the resulting void space, with the methane/propane configuration being taken from a simulation of a bulk methane/propane mixture at 277 K and 4 kbar. Thus, in total, the simulation box contained 408 water, 248 methane, and 144 propane molecules.

A 5-ps MD simulation was then performed using 3-D periodic boundaries and keeping the position of the water molecules fixed; this was followed by a further 5 ps in which all molecules were mobile, but the mass of the water molecules had been increased by a factor of 10. The final configuration was used as the starting point for a 200 ps simulation of an uninhibited hydrate surface at 277 K and 4 kbar. A previous study[28] had found this thermodynamic state to be in the middle of the hydrate-stable region of the phase diagram (for these intermolecular potentials) and shown that 200 ps was long enough to identify and characterize instability in the hydrate film.

The inhibited system was constructed from the initial configuration of the uninhibited system by inserting one TBAPS molecule on the hydrocarbon side of the interface. Those methane or propane molecules that overlapped with the TBAPS were then removed, the hydrate and TBAPS frozen and a 5-ps *NVT* simulation used to allow the fluid phase to relax. A 200-ps *NVT* simulation was then performed for subsequent analysis. The number of methane and propane molecules removed was determined by trial and error to give a pressure of 4 kbar in the subsequent production run, so that the final system contained 1 TBAPS, 408 water, 241 methane and 140 propane molecules.

3.2 Results. A number of analysis techniques have been employed to investigate how the inhibitors interact with the gas hydrate surface and the resultant effect upon gas hydrate surface structure. In this paper we focus on the structural effect of the KI on the surrounding water, as revealed in the radial distribution functions (RDFs). Some results on the translational and rotational motion of water solvating the KI are also presented.

In the [111] direction, a type II hydrate can be constructed by stacking equivalent 10 Å layers; the successive layers are offset in an ABC stacking pattern to give a crystallographic translational repeat distance of 30 Å ($= \sqrt{3} \times 17.3$ Å, where 17.3 Å is the length of the cubic crystal unit cell). Thus, for analysis, the hydrate film was divided into 6 slices parallel to the surface, each 5 Å thick. The inhibitor was added close to the top slice (number 6) and so it is this region that forms the focus of the present paper. We note in passing that the other 5 slices showed no signs of being affected by the presence of the inhibitor on the time scale of these simulations. The middle 4 slices exhibited a stable structure that was indistinguishable from the bulk hydrate (consistent with the phase behavior observed in earlier calculations[28]) and slice 1 showed signs of surface-melting that were the same with and without the inhibitor near the other surface. As a result, the following discussion is focused solely on the inhibited surface (slice 6).

Radial distribution functions (RDFs) for water within the hydrate surface (slice 6) are given in Figure 2, where a subscript W is used to denote an atom that is part of a water molecule. In general, these plots show small but significant differences between the inhibited and uninhibited surfaces. The O_W-O_W distribution shows a slight decrease in the first peak height and a small outward shift in the second peak in the presence of TPABS, but otherwise very similar structures. In both cases, there is little similarity with the hydrate RDFs evident in the middle of the hydrate film. More variation is seen in the H_W RDFs, with the inhibitor surface showing significantly less structure than the uninhibited surface. The observed differences are consistent with water hydrogen bonding to the sulfonate group rather than to other water molecules.

The RDFs presented in Figure 2 are averaged over all of the water molecules in the surface. Most of these molecules are

(21) Smith, W.; Yong, C. W.; Rodger, P. M. *Molecular Simulation* **2002**, *28*, 385.
(22) Berensden, H. J. C.; Postma, J. P. M.; van Gunsteren, W. F.; Hermans, J. *Intermolecular Forces*; Pullman, B., Ed.; D. Reidel Publishing Co.: Dordrecht-Holland, 1981, 331.
(23) Jorgensen, J. L.; Madura, J. D.; Swenson, C. J. *J. Am. Chem. Soc.* **1984**, *106*, 6638.
(24) Westacott, R. E.; Rodger, P. M. *Chem. Phys. Lett.* **1996**, *262*, 47; Rodger P. M. *J. Phys. Chem.* **1989**, *93*, 6850.
(25) Brooks, B. R.; Bruccoleri, R. E.; Olafson, B. D.; States, D. J.; Swaminathan, S. *J. Comput. Chem.* **1983**, 4, 187.
(26) Ewald, P. *Ann. Phys.* **1921**, *64*, 253.
(27) McMullan, R. K.; Kvick, A. *Acta Crystallogr. B* **1990**, *46*, 390.
(28) Storr, M. T. *Computer Modelling of the Mode of Action of Gas Hydrate Kinetic Inhibitors*, Ph.D. Thesis, University of Warwick 2001; Storr, M. T.; Rodger, P. M., manuscript in preparation.

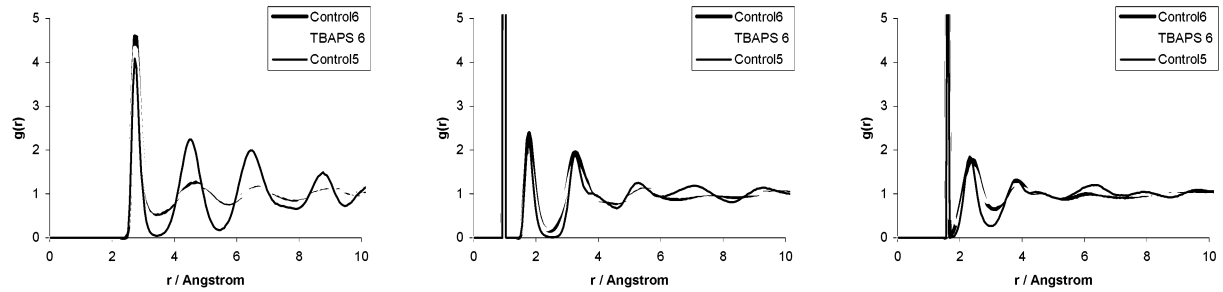

Figure 2. RDFs for O_W-O_W (left), O_W-H_W (middle) and H_W-H_W (right) for the uninhibited surface (thick, black) and inhibited surface (thick, gray); the subscript "W" is used to indicate an atom within a water molecule. The RDFs for slice 5 (just below the hydrate surface and containing stable hydrate) is given for comparison (thin, black).

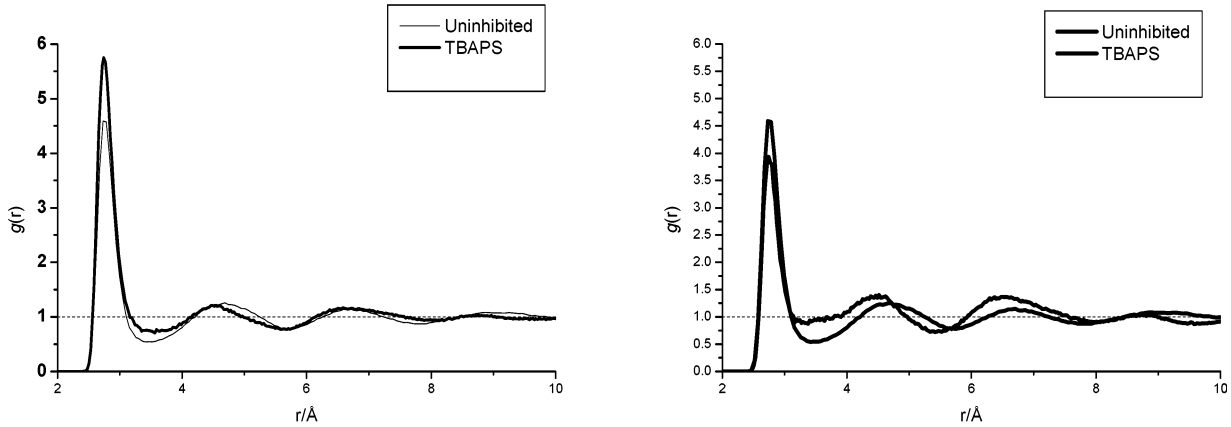

Figure 3. O_W-O_W RDFs for the surface slice where at least one O_W is adjacent to a methyl carbon (left) or a sulfonate oxygen (right) atom on the inhibitor (grey lines). The black line is the analogous distribution for water not near the inhibitor, as calculated from the uninhibited system.

not adjacent to the inhibitor and so these RDFs will not be particularly sensitive to the effect of the inhibitor on the surrounding water. To overcome this, RDFs have been calculated specifically for those water molecules that do solvate the various constituent atoms within the inhibitor. RDFs for water solvating the methyl group of the butyl chains, or the oxygen atom of the sulfonate group, are depicted in Figure 3. These two RDFs were chosen because they represent 'classic' hydrophobic and hydrophilic moieties respectively and should help to identify the extremes in behavior of the inhibitors.

It is clear from Figure 3 that the inhibitor does markedly affect the water structure, and that its effect is opposite around the hydrophobic and hydrophilic groups. Around the hydrophobic methyl groups there is an increase in the first peak height, which is usually considered to be indicative of stronger hydrogen bond formation between the water molecules. The second peak is also sharper and occurs at a shorter distance than is seen on the uninhibited surface, although this effect is relatively small. Overall, the aqueous environment of the methyl groups appears to be compatible with the structure of the hydrate surface, though with some localized strengthening of the hydrogen bond network. A considerably different picture is seen around the hydrophilic sulfonate oxygen atoms, however. The first peak is considerably smaller than for the uninhibited system and the minimum between the first two peaks is very flat with a minimum value close to 1 (the bulk density). Further, the second, and particularly third, peaks are much stronger than for the uninhibited surface, and are located at shorter distances. These results suggest that the sulfonate group enhances water structure in the mid-long range, but in a way that is not compatible with the hydrate.

Selected water-inhibitor RDFs are presented in Figure 4; we have adopted the notation X−W, where X indicates either a methyl carbon (C) or a sulfonate O atom (O_S), and W is either O_W or H_W. As a reference, it is convenient to compare the O_S-W RDFs with those for O_W-W calculated for an uninhibited system, since both O_S and O_W are hydrogen bond acceptors. The O_S-O_W RDF shows a pronounced contraction in the water first solvation shell compared with O_W-O_W: the first peak moves to shorter distances than for the uninhibited case and there is a reduction in the first peak height. The second and third peaks are also at shorter distances, but their heights are larger than for the uninhibited case; this is the same trend discussed above for water in the vicinity of the sulfonate (Figure 3) and suggests that the sulfonate generates a new hydrogen-bond network structure that propagates over several solvation shells. The O_S-H_W RDF also indicates strong hydrogen bonding, with a peak at 1.6 Å—shorter than found in the control. Three more prominent peaks occur in the range 2−6 Å, again indicating a high degree of solvent structure around the sulfonate group. In contrast, the solvent distribution around the methyl groups exhibits little structure, with the RDF remaining close to the equilibrium value of 1. RDFs were also calculated for the distribution of water around N (see the Supporting Information); these indicated that the N is inaccessible to the water, with no significant water density within 3.5 Å and no peaks within 6 Å. We note that this behavior is incompatible with a mechanism conjectured for AA activity in quaternary alkylammonium salts in which the N is suggested to replace a water molecule within the hydrate lattice.[29]

The simulations have also been analyzed for dynamical effects arising from the inhibitor. Various time correlation functions

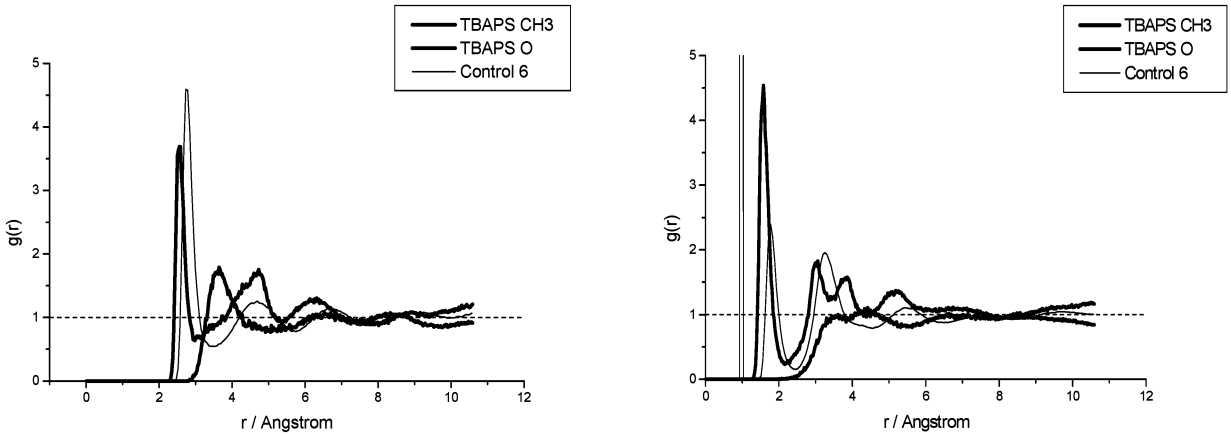

Figure 4. $X-O_W$ (left) and $X-H_W$ (right) RDFs, where X is a methyl carbon (C, thick black), or sulfonate oxygen (O_S, thick gray), atom in the inhibitor; O_W-O_W and O_W-H_W RDFS (thin black) are shown for comparison.

Table 1. Diffusion Coefficients for the Oxygen Atom, and Rotational Lifetimes for Motion Parallel to and Perpendicular to the Dipole Moment, of Water Molecules Confined within the Solvation Sphere of the Methyl Group and the Oxygen Atom of the Sulfonate Group

molecule	group	$D(O_W)/Å^2ps^{-1}$	$\tau_{2\|\|}$/ps	$\tau_{2\perp}$/ps
TBAPS	CH3	0.16	0.57	0.58
TBAPS	O	0.21	0.60	0.67

(TCFs) were calculated for water molecules that started and remained within the inhibitor solvation shell and compared with the corresponding functions calculated for water in the uninhibited system. Approximate transport coefficients were then obtained from the early time behavior of these TCFs. We note that the transport coefficients are more correctly defined from the long-time behavior of the TCFs, but for times longer than the residence time of a water molecule within a given solvation shell, the TCF will cease to probe the dynamics of the specified environment. The use of the early-time behavior (0−2 ps) is therefore justified to give a relative indication of the mobility of water in the different environments.

Values for the diffusion coefficient and rotational lifetimes of water in various environments are listed in Table 1. The diffusion coefficients were obtained from the slope of the mean square displacement of O_W atoms. Rotational lifetimes were obtained from the slope of semilog plots of the Legendre angular correlation function: $P_2(\cos <\boldsymbol{e}(0).\boldsymbol{e}(t)>)$, where P_2 is the second Legendre polynomial, $\boldsymbol{e}(t)$ is some vector property of a water molecule at time t, and the $<>$ denotes an ensemble average. We present results for $\boldsymbol{e}$ being (i) the water dipole vector, denoted $_{||}$, and (ii) a vector perpendicular to this and lying within the plane of the water molecule, denoted $\perp$. In general, these results indicate that water is less mobile around the hydrophobic methyl group than it is around the hydrophilic sulfonate group. Although the differences can be quite small (5−25%), this trend is consistent with the suggestion from the RDF analysis that the hydrogen bond network in the water is strengthened around the methyl groups, but weakened around the sulfonate. These trends are also consistent with those observed in aqueous alcohols.[30]

Table 2. Summary of Inhibitor Mixtures Used

inhibitor mixture concentration/wt % water					
TBAPS	PVP	notation		experiments	
0	0	C	THF hydrate	C_2H_6 hydrate	morphology
0.1	0	T_1		C_2H_6 hydrate	
0.5	0	T_5	THF hydrate	C_2H_6 hydrate	morphology
0.4	0.1	T_4P_1	THF hydrate		
0.3	0.2	T_3P_2	THF hydrate		
0.25	0.25	$T_{2.5}P_{2.5}$	THF hydrate		
0.2	0.3	T_2P_3	THF hydrate		
0.1	0.4	T_1P_4	THF hydrate		
0	0.5	P_5	THF hydrate		morphology

4. Experimental Characterization of KI Activity

4.1 Methods. Synthesis of TBAPS. TBAPS[31] was prepared by a modification of a literature procedure.[32] Tributylamine (200 mL, 0.84 mol) and 1,3-propanesultone (20 g, 0.16 mol) were dissolved in 1,2-dichloroethane (200 mL) and allowed to stir under nitrogen for 3 days. A white precipitate formed (45 g, 91% yield), which was filtered and washed with petroleum ether. The product was recrystallized from a mixture of chloroform, petroleum ether and acetone: mp 172−173 °C; ν_{max} (nujol mull), 1495, 1203, 1035; δ_H (300 MHz, $CDCl_3$), 1.02 (9H, t, CH_3), 1.44 (6H, m, CH_2CH_3), 1.72 (6H, m, $CH_2CH_2CH_3$), 2.20 (2H, m, CH_2CH_2S), 2.93 (2H, t, CH_2S), 3.23 (6H, m, CH_2CH_2-CH_2CH_3), 3.75 (2H, m, CH_2N); δ_C (100 MHz, $CDCl_3$), 13.47, 18.64, 19.57, 23.61, 47.14, 57.91, 58.53; *m/z* (CI+), 308 (15%) $[M+H]^+$, C 58.18%, H 10.74%, N 4.44%, ($C_{15}H_{33}NSO_3$ requires C 58.59%, H 10.82%, N 4.56%).

Inhibitors. Subsequent experiments were carried out with (i) TBAPS, (ii) poly(vinylpyrrolidone) (PVP, Flukka, 40 000 M. W.), and (iii) mixtures of these two inhibitors. In most cases, the inhibitor or inhibitor mixture was present at 0.5 wt % water, although one experiment with ethane hydrate used just TBAPS at 0.1 wt % water. A summary of the different inhibitor mixtures is given in Table 2 together with the notation that will be used within this paper to refer to the different systems.

Inhibition of THF Hydrate. Full details of the experimental procedure are described elsewhere,[33,34] and so the procedure is

(29) Frostman, L. M.; Przybylinski, J. L. *Proc. SPE Int. Symp. Oilfield Chem., Houston* **2001**, 230; Frostman, L. M.; Downs H. *2nd Int. Conf. Petroleum and Gas-Phase Behaviour and Fouling, Copenhagen* 2000.
(30) Fidler, J.; Rodger, P. M. *J. Phys. Chem. B* **1999**, *103*, 7695.
(31) Linfield, W. M.; Abend, P. G.; Davis, G. A. *J. Am. Oil Chem. Assoc.* **1963**, *40B*, 114.
(32) Brunelet, T.; Jouitteau, C.; Gelbard, G. *J. Org. Chem.* **1986**, *51*, 4016.
(33) Jussaume, L.; Canselier, J. P.; Monfort, J. P. *Proceedings AIChE Spring National Meetin*g, Houston, USA, 14−18 March, 1999.

only summarized here. Up to eight 8-mL test tubes were each filled with 7.5 mL of solution. The stock solution was a 20 wt % solution of tetrahydofuran (THF) in water. To this was then added an inhibitor at 0.5 wt % water. A temperature probe was attached to each test tube and the temperature monitored as a function of time. The system was then cooled to 2 °C at 0.2 °C min^{-1} and then kept at 2 °C for the duration of the experiment. The test tubes were subjected to continuous agitation once the temperature reached 6 °C. Each test tube was monitored until the onset of THF hydrate formation, as evidenced by a sudden increase in the temperature of the mixture (due to the enthalpy of crystallization). The induction time for the formation of THF hydrate, t_{ind}, was taken to be the time between the mixture reaching 2 °C and the start of the temperature spike due to crystallization.

Morphology of THF Hydrate. These experiments were performed using the method described by Zanota.[35] A fixed window quartz crucible was filled with 0.2 mL of a solution containing THF (20 wt % water), water and either TBAPS (0.5 wt % water) or PVP (0.5 wt % water); a control system with just THF (20 wt % water) and water was also used. The fixed window quartz crucible was then mounted onto an Olympus BX50 microscope stage fitted with a Linkam temperature regulation system accurate to 0.1 °C. The stage was held at 6 °C for 5 min to allow thermal equilibrium to be achieved; once this had been achieved, the stage was cooled to 2 °C and maintained there until the experiment was finished. The experiment was recorded throughout via a Sanyo video camera attached to the microscope, and digital images of morphologies extracted from the resulting movies.

Growth Kinetics of Ethane Hydrate. Experiments were carried out using the method described by Monfort and co workers[34,36] A high-pressure reactor was charged with deionized water and the system pressurized with ethane and maintained at 12 bar and 8 °C. The system was then left to equilibrate, during which time some ethane dissolved in the deionized water. Once saturation and thermal equilibrium had been achieved the system was closed.

A series of hydrate formation/decomposition cycles were then carried out. The system was held at 8 °C for 15 min, then cooled to 4 °C at 0.13 °C $minute^{-1}$ then held at 4 °C until hydrate equilibrium was achieved. Once the pressure stabilized following hydrate formation at 4 °C the system was heated back to 8 °C at 0.13 °C $minute^{-1}$ and held at this temperature for 15 min. Although the first cycle gave significantly longer induction times, the second and subsequent cycles were found to be reproducible; this is consistent with the hydrate memory effect reported by other workers.[37] A complete cycle took about 60 min to complete.

A small sample of liquid (80 mL) was then removed from the reactor vessel and replaced by 60 mL of inhibitor solution followed by a 20 mL water rinse. The concentration of the added inhibitor solution was chosen to give the target concentration in the reactor. A new series of formation/decomposition cycles was undertaken to determine the activity of the inhibitor. This procedure was then iterated to study successively higher inhibitor concentrations—all acting on the same water/ethane sample.

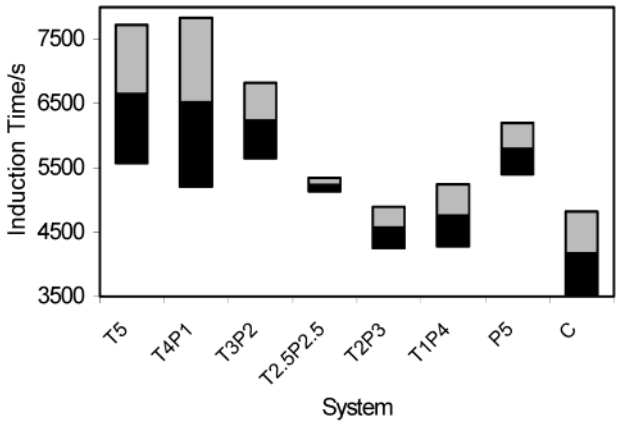

Figure 5. Plot of average induction time vs system. The column heights indicate ± one standard deviation of the mean. The system notation is defined in Table 2.

The reactor vessel was attached to a granulometer and fed by a continuous flow of liquid from the (stirred) reactor vessel throughout the experiment. This enabled measurement of the particle size distribution in situ as a function of time. Extreme care was taken to ensure that no contaminants were introduced into the reactor vessel. The induction time was then defined to be the time from when the temperature in the reaction vessel first reached 2 °C to the first appearance of particles bigger than 2 μm (the resolution of the granulometer). The subsequent time dependence of the particle size distribution was then analyzed to determine the nucleation rate, R_n and the growth rate, R_g of hydrate crystals.[38] Reactor pressure was also monitored as a function of. time, from which it was possible to determine gas consumption rates for hydrate formation.

4.2 Results. THF Hydrate. Results from our experiments on the effectiveness of TBAPS and PVP in inhibiting the crystallization of THF hydrate experiments are presented in Figure 5. The figure depicts both the average and standard deviation of the mean of the observed induction time, and is derived from 4 to 8 equivalent tests for each system.

It is clear from Figure 5 that, under these conditions, TPAPS and PVP both induce a significantly longer induction time than is found in the uninhibited system. Most promisingly, the proposed new inhibitor, TBAPS, appears to delay the onset of hydrate formation even more effectively than one of the established commercial inhibitors, PVP, although a *t*-test indicates that this improvement is significant only at about a 90% level.

The experiments with the mixed inhibitor systems were performed to determine whether there was any synergism between TBAPS and PVP. Synergism is a positive deviation from a simple linear relationship between the two pure systems, i.e. mixtures of TBAPS and PVP would be more active than either TBAPS or PVP on their own. However, Figure 5 indicates that the opposite effect is found with TBAPS/PVP mixtures, with the experiments giving a U-shaped curve with a *minimum*

(34) Jussaume, L. *Etude d'inhibiteurs cinétiques d'hydrates de gaz: néthods expérimentales et modélisations numériques*, Ph.D. Thesis. INP Toulouse, 1999.
(35) Zanota, M. L. *Formation d'hydrates dans les systèmes quaternaires eau/THF/huile/tensioactifs: effets anti-agglomérant des tensioactifs*, Ph.D. Thesis, UPPA 2001.
(36) El Hafaia, T.; Monfort, J. P. *Proceedings AIChE Spring National Meeting*, Houston, USA, 14−18 March, 1999.
(37) Moudrakovski, I. L.; Sanchez, A. A.; Ratcliffe, C. I.; Ripmeester, J. A. *J. Phys. Chem. B* **2001**, *105*, 12 338; Takeya, S.; Hori, A.; Hondoh, T.; Uchida, T. *J. Phys. Chem. B* **2000**, *104*, 4164.
(38) Monfort, J. P.; Jussaume, L.; El Hafaia T.; Canselier, J. P. *Ann. N. Y. Acad. Sci.* **2000**, *912*, 753.

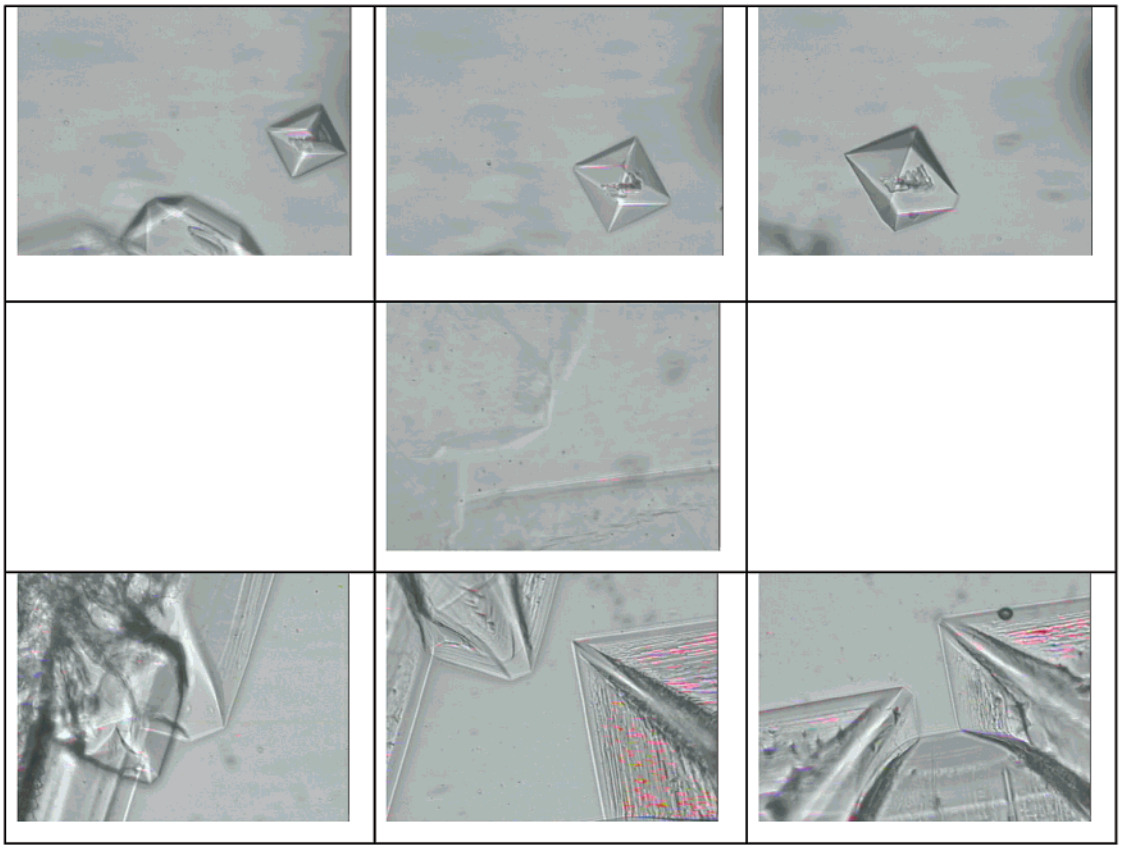

Figure 6. Sample images from experiments on the morphology of THF hydrate. Top: THF hydrate (C); Middle: THF hydrate with 0.5 wt % PVP ($P_{0.5}$); Bottom: THF hydrate with 0.5 wt % TBABS ($T_{0.5}$).

for the T_2P_3 mixture. Thus we find that the mixtures are less effective than either of the pure inhibitors (T_5 and P_5) at delaying the crystallization of THF hydrate.

The morphology studies confirm that the TBAPS does affect hydrate growth. A selection of the images obtained during the growth studies are presented in Figure 6. In the absence of an inhibitor the THF hydrate forms octahedral crystals. This is consistent with the results obtained for the crystal growth of THF hydrate in uninhibited systems from previous studies.[39,40] In the presence of PVP, however, the hydrate grows as thin, planar crystals, to the extent that it is very difficult to observe the crystals, which are almost transparent. This is again consistent with previous results obtained for the crystal growth of THF hydrate in the presence of PVP.[39,40] The morphology observed in the presence of TBAPS is more complex than in the other two cases. There is evidence of deformed, and particularly elongated, octahedra. These are often associated with the growth of planar sheets extending out from the edges of the elongated octahedra, with the sheets being considerably thicker than in the PVP system, and showing surface rippling. We conclude that TBAPS is effective in changing the morphology of THF hydrate crystals, and that it does so in a manner that is quite different from that found with PVP.

Ethane Hydrate. The results of the experiments on the nucleation and growth of ethane hydrate are listed in Table 3. It is immediately clear that TBAPS is effective in delaying the onset of hydrate formation, although its effect on the subsequent growth of hydrate crystals is less obvious.

Table 3. Kinetics of Formation of Ethane Hydrate: Induction Time, t_{ind}, and Rates of Nucleation, R_n, Crystal Growth, R_g, and Gas Consumption, R_c[a]

inhibitor	t_{ind} / s	R_n / ml^{-1} min^{-1}	R_g / μm min^{-1}	R_c / bar h^{-1}
C	−90 (32)	1439 (1031)	1.56 (2.18)	0.55 (0.10)
T_1	1705 (422)	89 (−)	0.61 (0.23)	0.63 (0.20)
T_5	2678 (231)	116 (13)	0.86 (0.25)	0.51 (0.08)

[a] Values in parentheses are the standard deviation of the mean. Inhibitor notation defined in Table 2.

Table 3 gives both induction times and nucleation rates. The induction time is the time to the first appearance of hydrate crystals, measured from the time when the reactor first reached the target temperature of 4 °C. The negative value in the uninhibited simulation indicates that the first crystal typically appeared during the cooling stage, with −90 s corresponding to about 4.2 °C; at 12 bar, the temperature for three-phase equilibrium between water, ethane and hydrate is 8 °C. In contrast, the systems with TBAPS persist for 30−45 min at 4 °C (a sub-cooling of 4 °C). t_{ind} does increase with concentration of TBAPS, but the effect does not appear to be linear, with a 5-fold increase in concentration leading to a 50% increase in induction time.

Two things must be remembered in assessing these induction times. The first is that this is a first generation inhibitor, and it must be expected that subsequent optimization of this new lead compound will substantially increase its activity. The second point is that this experiment is designed to exploit the memory effect in hydrate formation,[37] whereby second and subsequent

(39) Larsen, R.; Knight, C. A.; Sloan, E. D. *Fluid Phase Equilibria* **1998**, *151*, 353.
(40) Makogon, T. Y.; Larsen, R.; Knight, C. A.; Sloan, E. D. *J. Crys. Growth* **1997**, *179*, 258.

crystallization cycles occur much more rapidly and reproducibly than the first cycle. Thus, much longer induction times would be expected in real applications because these would have no residual order from earlier hydrate crystallization events to facilitate the nucleation. In fact, the performance of TBAPS again appears to be comparable with that of PVP, which has been shown to extend the induction time (compared with the uninhibited system) for ethane hydrate in the same experimental rig by about 5600 s at 4 °C and 10.7 bar (i.e., at a smaller subcooling than used in our tests).[34]

The nucleation rates have been determined from the rate at which new hydrate particles appear once crystallization has begun These confirm that TBAPS is effective in suppressing nucleation: there is more than a 10-fold decrease in nucleation rate in the presence of TBAPS compared with the uninhibited system. Once again, there does not appear to be a strong increase in activity with inhibitor concentration under the experimental conditions, although the experimental uncertainties make detailed comparison of the two inhibited systems difficult.

In contrast to the nucleation rate, TBAPS appears to have little effect on the subsequent growth of hydrate. The gas consumption gives an indication of the amount of hydrate formed, and so the rate of gas consumption is a direct measure of hydrate growth rates; our experiments give essentially the same growth rate in all three systems. Similar results are seen with the R_g, which measures the rate at which the average diameter of a hydrate crystal grows. The data for R_g suffer from a poor signal-to-noise ratio and so it is difficult to be definitive about any trends, but may be that TBAPS leads to a halving of the rate at which the crystal radius increases.

5 Conclusions

In this paper we have presented a combined theoretical and experimental study of the activity of a new form of kinetic inhibitor of gas hydrate formation: tributylammoniumpropylsulfonate (TBAPS). The inhibitor was identified in a computational screen on the basis of its unusual surface adsorption behavior. Subsequently, molecular dynamics (MD) simulations were used to characterize the effect of TBAPS on a hydrate/natural gas interface. The simulations showed that TBAPS is bifunctional. The hydrophobic end of the molecule has an aqueous solvation structure that is compatible with the structure of the hydrate surface but with a slight strengthening of the water−water hydrogen bonding. In contrast, the sulfonate group induces a new water structure that is not compatible with the hydrate and that propagates over several solvation shells.

TBAPS was then synthesized and tested in existing experimental rigs for its effect on both ethane and THF hydrate formation. In both THF and ethane hydrate, TBAPS was shown to delay the onset of hydrate formation as effectively as poly(vinylpyrrolidone) (PVP); comparative tests with more active commercial inhibitors are in progress.[16] The TBAPS also induced complex changes in the morphology of THF hydrate crystals, with the crystal habit changing from octahedral in the absence of any inhibitor to elongated octahedra with extensive planar sheets growing from the octahedral edges in the presence of TBAPS.

We conclude that this new KI constitutes a promising lead compound for a new class of kinetic hydrate inhibitors, and extensive work is already underway to generate second generation inhibitors from this lead.

Acknowledgment. The authors wish to thank Dr M. L. Zanota for help with the morphology experiments. This work was supported by the EPSRC through a postgraduate studentship.

Supporting Information Available: Calculated RDFs for the distribution of water around N. This material is available free of charge via the Internet at http://pubs.acs.org.

JA035243G